Impact Behaviour Analysis of a Passive Compliant Unit for Active Space Debris Removal

Maxime Hubert Delisle[1], Xiao Li[1], Barış C. Yalçın[1], Miguel Olivares-Mendez[1] and Carol Martinez[1]

***Abstract*— The exponential growth of space debris in Low-Earth Orbit (LEO) has led Active Debris Removal (ADR) systems to be declared by space agencies as a viable solution for ensuring safe space activities. The main capturing systems are designed for large specific cooperative satellites, which leads to expensive one-to-one solutions. However, several uncooperative small debris remain in LEO. These can still be a great threat for future space missions. By integrating active and passive compliance parts, the studied concept set a closer step towards a one-to-many solution. This Hybrid-Compliant system can help dissipate the impact energy, increasing the space system's autonomy, and consequently help capture a broader range of space debris. This paper focuses on building a program simulating the mechanical behaviour of the system's Passive Compliant Unit (PCU) during an impact with a flat-surface debris and comparing it with experimental data. A presentation of the PCU concept, and its testing prototype, is first introduced. Then, the simulation model is presented through the equations and workflows involved. After that, an experimental testing procedure is proposed, as the generated data will finally help compare with the model. A discussion about future improvements of the model and further works concludes this paper.**

I. INTRODUCTION

For more than 60 years of space activities, the number of in-orbit objects has increased [1]. More than 130 million debris objects are in orbit [3]. With the number of space debris growing exponentially [2], critical problems for ongoing and future space missions have higher probability to occur. ADR is thus required [4] so that the global space environment can avoid the unwanted foreseeable scenarios. The main issue with space debris is that most targets are uncooperative for capturing [5], and they do not include specific handles or markers to make the task easier [6]. Moreover, each debris has its unique geometry, velocity, and material [7]. Hence, capturing autonomously and harmlessly uncooperative objects is critical, and demands reliability, robustness, and control at the impact. Capturing debris can imply different kind of interactions; an Energy-Transfer Classification (ET-Class) was proposed in [8]. The *Impact Energy Dissipation (ET2)* class implies a capture with a decrease of energy at the first impact. Yet, the most crucial problem regarding rigid capturing methods keeps still, since rigidness lacks appropriate impact energy dissipation in a frictionless environment. As a result, both academia and industry leaders are inclined to focus on flexible capturing methods rather than rigid capturing methods [9]. For instance, Shape Memory Alloys (SMA), such as MEDUSA [13], and pneumatic capturing mechanisms are nowadays part of the most popular flexible mechanisms [10] [11] [12]. They can be categorised in the *ET2* category as capturing mechanisms of this class decrease the impact energy of the debris at the very first contact. In addition, a Hybrid-Compliant System for Soft Capture of Uncooperative Space Debris has been proposed [18] in our previous work, combining an Active Compliance Unit (ACU), electronically controlled, and a Passive Compliance Unit (PCU), naturally compliant with torsional springs. This versatile system of class *ET2* [8], is displayed in Figure 1. This new system targets a wide range of small debris, enabling a profitable autonomous one-to-many solution. In contrast to previous concepts, the mechanism's compliance is hybrid, taking advantage, at its interface with the debris, of a bio-inspired dry adhesive technology [17] [16] [19], ensuring adequate contact time, and successfully helping capture a broader range of space debris.

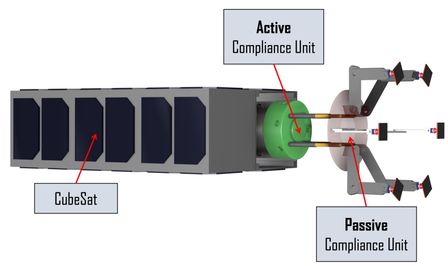

Fig. 1. Hybrid-Compliant System Concept View.

This paper proposes to investigate further the mentioned design, by modelling the PCU's behaviour with:

- The Concept and Prototype of the PCU (Section II);
- A simulation model of the PCU recreating the subsystem behaviour at the impact with a flat-surfaced free-floating debris (Section III);
- Experimental tests to assess the proposed model (Section IV).

II. THE PASSIVE COMPLIANT UNIT (PCU)

Capturing uncooperative space debris demands high reliability. Softening the impact will ensure that the debris is not pushed away and the soundness of the system. To guarantee this soft capture, the hybrid-compliant system integrates a passive compliance architecture. Figure 1 presents a conceptual close-up view of this hybrid mechanism. It

[1]The authors are with the Space Robotics (SpaceR) Group of the Interdisciplinary Centre for Security, Reliability and Trust, University of Luxembourg, L-1855 Luxembourg, Luxembourg maxime.hubertdelisle@uni.lu

comprises two crucial parts: the Active Compliance Unit (ACU), with tunable stiffness, and the Passive Compliance Unit (PCU), with a permanent stiffness. Together they form the Soft Capture Unit (SCU) of adjustable stiffness of our capturing mechanism.

As this paper centers on the PCU, a comprehensive overview of its design is presented below, while the ACU falls beyond the scope of this study. For more details, please refer to [18].

A. Design of the PCU

The PCU, as shown in Figure 2 (a), has two main functions: to ensure a softer impact with the debris, as well as to adhere to the debris surface, preventing it from moving away. This unit comprises three parts: articulated legs, spherical joints, and adhesive pads. This part is the first of the whole system to encounter the target's surface.

Each articulated leg includes a torsional spring in order to create a revolute joint. Thus, the passive compliance and flexibility feature is made possible. The choice of adding torsional springs is for two reasons; a softer impact and better safety concerns. The torsional springs' stiffness determines the PCU's maximum deflection in the axis of capture. This parameter plays an important role in the overall hybrid compliance.

Spherical joints link the articulated legs to the adhesive pads. They give the pads additional mechanical degrees of freedom, thus an improved adaptability and alignment to the debris surface, as this can be determining the performance of the dry adhesives [15].

At the tip of each leg, a gecko-inspired dry adhesive [14] component is integrated as a thin layer under the pads. This dry, yet sticky, material is activated by applying a shear force [15]. Combined with a contact [16] or a proximity sensor, the adhesives can be activated accordingly. The shear force is created thanks to the active shrinkage of the legs towards the capture axis. No additional normal force is required to adhere. To that extent, getting a space-tested [17] dry adhesive activated by shear force is the most suitable solution for catching space debris more reliably.

B. PCU Early-Stage Prototype

To start testing the PCU's feature in the lab environment, an iterative process of prototyping is required. This section provide a brief description of the prototype architecture as well as its purpose. The goal of this prototype is to test and assess specific features of the overall hybrid-compliant system; testing the passive compliance capabilities, as well as the adequate timing of activation of the dry adhesive material and its actual efficiency. This paper only focuses on the passive compliance capabilities of the PCU.

The prototype is composed of two different parts, as displayed on Figure 2 (b): the PCU itself, and the Electronics & Control Unit (ECU). Unless specified, each part of the prototype is 3D printed.

The prototype of the PCU is made of three articulated legs, thoughtfully placed so that they can shrink towards the centre axis line of capture. Prototyping three legs provides the minimum significant number of legs to evaluate the behaviour of the proposed system. Each of these legs include a purchased torsional spring, made of steel, at their root joint; at the interface with the ECU. To determine their torsional spring rate, calculations has to be done [23]. Considering the spring parameters in I, equation 1 gives a torsional spring rate for one spring of $k_T = 0.053\,\mathrm{N\,m\,rad^{-1}}$.

Sign	Value	Description
D_m	$6.0 \times 10^{-3}\,\mathrm{m}$	Mean Coil Diameter
d	$0.8 \times 10^{-3}\,\mathrm{m}$	Wire Diameter
E	$200 \times 10^{9}\,\mathrm{Pa}$	Young's Modulus
N_a	4	Number of Active Turns

TABLE I
SPECIFICATIONS OF THE TORSIONAL SPRING

$$k_T = \frac{d^4 E}{64 D_m N_a}, \tag{1}$$

The ECU plays the role of controlling and giving power to the electronic elements required for the PCU to work. It comprises of an Arduino board, a breadboard, a slot for a portable battery, a thoughtfully-placed SG-90 servo-motor, and a custom slot for an HR04 proximity sensor. The former is used to pull the ropes required for creating the shear force with the dry adhesive, while the latter checks for the contact with the flat debris' surface. Those two features are not tested in the scope of this paper.

III. PCU IMPACT BEHAVIOUR SIMULATION MODEL

The simulation model is built from scratch in the MATLAB environment; so that it is tailor-made for the designed system presented in Section II.

The main goal of the simulation model is to assess that, regarding the parameters of the impact, it would stay safe and sound; the longitudinal deflection of the PCU's articulated legs doesn't reach its geometrical design limit of $20 \times 10^{-3}\,\mathrm{m}$. To do so, the simulation outputs the graph of the longitudinal deflection over time for the PCU's articulated legs, as well as the longitudinal limit to not reach.

A. Model variables

This model takes as inputs two variables that can be either extracted experimentally, or arbitrarily taken: the impact force at peak $F_{i,Peak}$, in N, and the time of collision t_c, in s. In order to estimate the longitudinal deflection out of the torsional springs under an impact force $F_{i,Peak}$, a series of calculation has to be conducted.

First, the torque applied to the spring has to be calculated. $F_{i,Peak}$ is applied on the pads of the PCU perpendicularly. However, the torsional spring's wire direction has an angle of $\alpha_{deg} = 30^\circ$ with regard to $F_{i,Peak}$ direction. So, to calculate the torque T applied to the spring, the perpendicular resultant of $F_{i,Peak}$ with respect to the spring wire direction has to

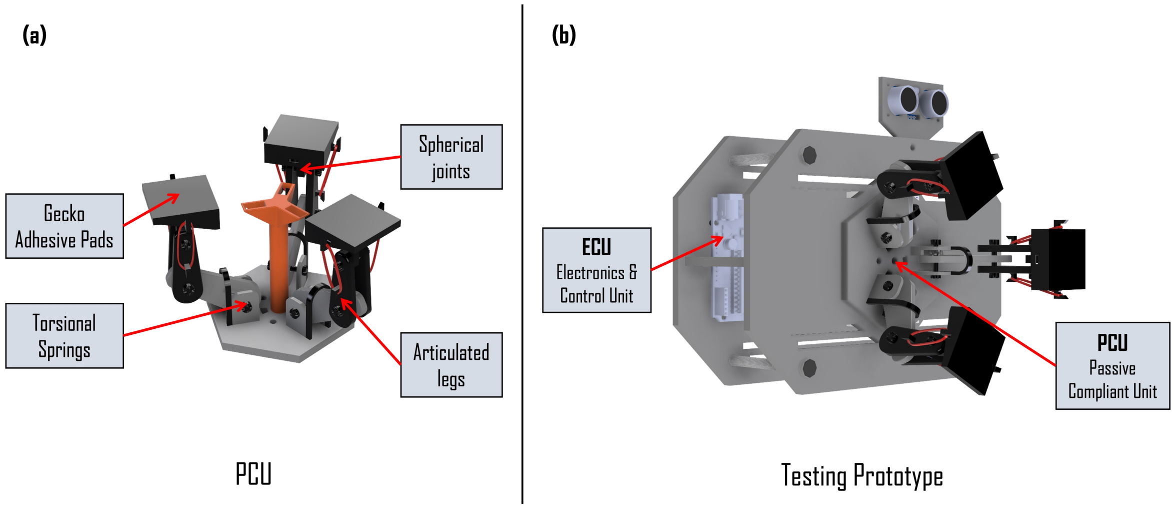

Fig. 2. (a) CAD of the PCU Prototype. (b) CAD of the Testing Prototype.

be taken into consideration, as in equation 2. In addition, $d_{arm} = 35 \times 10^{-3}\,\mathrm{m}$ denotes the distance between the point of application of the force and the centre of the spring.

$$T = F_{i,Peak} \cdot cos(\alpha_{rad}) \cdot d_{arm}, \tag{2}$$

Having the torque T, in $\mathrm{N\,m}$, and the torsional spring rate k_T, in $\mathrm{N\,m\,rad^{-1}}$, one can determine the angular deflection θ_{rad} of the torsional spring in rad with equation 3.

$$\theta_{rad} = \frac{T}{k_T}, \tag{3}$$

By knowing the angular deflection, one can geometrically deduct an estimation of the pad's linear deflection $\hat{\lambda}$, in m, as if an equivalent linear spring was placed below it. $\hat{\lambda}$ is directly linked to the deducted angular deflection θ_{rad}.

Now having the distance of which the pad deflect linearly, besides the impact force, a longitudinal stiffness k_L, in $\mathrm{N\,m^{-1}}$, can be approximated using equation 4,

$$k_L = \frac{F_{i,Peak}}{\hat{\lambda}}, \tag{4}$$

Finally, a linear damping coefficient b_L, in $\mathrm{N\,s\,m^{-1}}$, can also be approximated by considering, at first, a perfect case where the system is critically damped, meaning that the damping ratio $\zeta = 1$. Equation 5 gives a value for b_L,

$$b_L = \zeta \cdot 2\sqrt{k_L m_{PCU}}, \tag{5}$$

These values will be fed into the state-space model of the PCU in Section III-D, which will be excited by the adequate impact signal, in Section III-B.

B. Impact Signal Generation

To replicate the signal of the impact, the two model inputs, $F_{i,Peak}$ and t_c, will be used. A perfect collision can be described as a pulse by its amplitude and a very short time period. The signal starts at around $2\,\mathrm{s}$, and is generated using the *gensig* function on MATLAB. An example of the signal created can be seen on Figure 3.

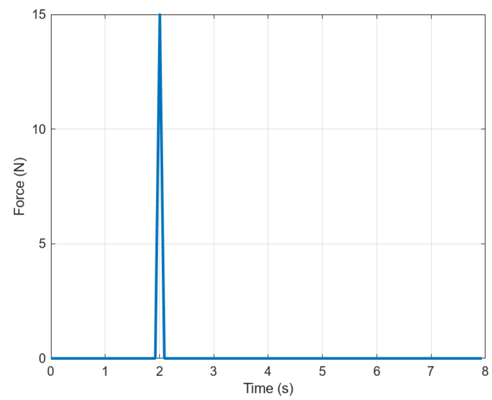

Fig. 3. Example of the signal created to replicate the pulse of the impact.

C. Equation describing the PCU behaviour

The PCU prototype is composed of three parallel spring-damper systems. It is possible to simplify the PCU spring-damper system to an equivalent system of three linear spring-damper systems in parallel, by summing their coefficients, as in equations 6 and 7. This can be adjusted depending on the number of legs the system have.

$$k_{eq,PCU} = k_{1,PCU} + k_{2,PCU} + k_{3,PCU}, \tag{6}$$

$$b_{eq,PCU} = b_{1,PCU} + b_{2,PCU} + b_{3,PCU}, \tag{7}$$

To model the behaviour of the PCU, a straightforward dynamic equation is used, as seen in equation 8,

$$m_{PCU}\ddot{y}(t) = u(t) - b_{eq,PCU}\dot{y}(t) - k_{eq,PCU}y(t), \tag{8}$$

with $y(t)$ being the longitudinal displacement of the PCU system over time and m_{PCU} the mass of the PCU system. The value of $u(t)$ is related to the impact force applied to the system over the time, which is in our case the impact force $F_i(t)$.

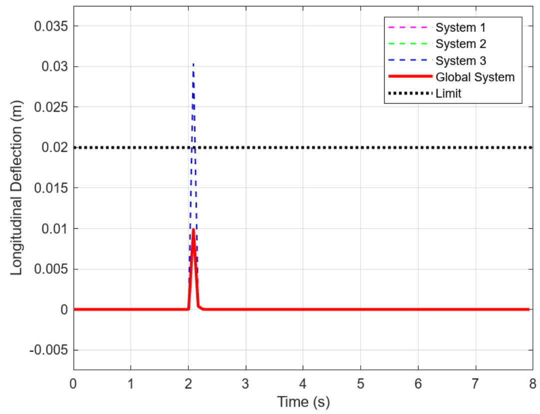

Fig. 4. Simulated linear deflection example.

D. State-Space Representation

The studied system can be modeled in a state-space representation as followed,

$$\begin{bmatrix}\dot{x}_1\\ \dot{x}_2\end{bmatrix} = A\begin{bmatrix}x_1\\ x_2\end{bmatrix} + B\left[u\right]$$
$$\left[y\right] = C\begin{bmatrix}x_1\\ x_2\end{bmatrix}$$

with x_1 being the position of the system, $x_2 = \dot{x}_1$ the velocity of the system, and $\dot{x_2} = \ddot{x_1}$ the acceleration of the system at a given time t, y the output vector, u the input vector and A, B, C, D being respectively the state matrix, the input matrix, the output matrix and the feedthrough matrix. As the system doesn't have a direct feedthrough, the D matrix is the zero matrix.

Regarding our global system, each state step of the dynamic system is expressed as,

$$\begin{aligned}\ddot{x}(t) = \frac{1}{m_{\text{PCU}}}u(t) - \frac{1}{m_{\text{PCU}}}b_{\text{eq,PCU}}\dot{x}(t)\\ - \frac{1}{m_{\text{PCU}}}k_{\text{eq,PCU}}x(t)\end{aligned} \tag{9}$$

so that the matrices A, B, C, D equals,

$$A = \begin{bmatrix}0 & 1\\ -\frac{k_{\text{eq,PCU}}}{m_{\text{PCU}}} & -\frac{b_{\text{eq,PCU}}}{m_{\text{PCU}}}\end{bmatrix}, \tag{10}$$

$$B = \begin{bmatrix}0\\ \frac{1}{m_{\text{PCU}}}\end{bmatrix}, \tag{11}$$

$$C = \begin{bmatrix}1 & 0\end{bmatrix} \tag{12}$$

The model outputs the linear deflection $\hat{L}$ in m endured by the pulse signal representing the collision with the debris over time, as displayed on the example on Figure 4. System 1, 2 and 3 refer to each leg separately, which, as they are the same, are superposed on the graph.

IV. EXPERIMENTAL VALIDATION

The Space Robotics Research Group (SpaceR) hosts a cutting-edge facility to test on-orbit scenarios at the University of Luxembourg, equipped with a flat epoxy floor and robotic floating platforms (FP) [22] emulating 2D free-floating objects in space. The FP can freely move in any direction on the ground floor plane, making it a realistic space debris floating in space under any contact forces. This laboratory is thus suitable for developing and assessing the novel Soft Capture system. By rigidly mounting the PCU prototype at the end effector of one UR10 robotic manipulator, a capturing approach path can be generated towards a flat debris surface attached to the top of one of the FP, as seen on Figure 5.

The experimentation aims to validate the accuracy of the PCU concept's simulation model. In other words, the model's linear deflection $\hat{L}$ value must be as close as possible to L found in the experimentation.

The initial state of the experimentation is known; the UR10 robot has the PCU prototype installed as its end-effector, the FP is turned on and stabilised in a free-flying mode with the flat debris surface mounted on it and at a known position in the lab. An OptiTrack camera system will sense the position of FP within the lab, as well as the relative position between the surface of the debris and the static part of the PCU. Moreover, a Force/Torque (F/T) sensor in the flange of the UR10 robot will allow to acquire the force and time of collision data from the impact.

The tests procedures follow these steps:

- The robotic arm initiates the path toward the debris surface mounted on top of the FP with a known velocity of V_{i_1}. The path that the robotic arm has to initiate is, at first, linear towards the debris. The floating platform is at first static.
- The PCU's feet and the debris surface enter in contact. The force $F_{i,Peak}$ and time of that collision t_c are sensed by the F/T sensor of the UR10 arm. The PCU's torsional springs are thus naturally solicited, and the OptiTrack sensors detect the distance to the debris surface. The linear deflection L in m is detected and recorded.
- The FP is pushed away freely, and its velocity V_{f_2} is acquired. The torsional springs come back to their initial state.

This data is then extracted, analysed and processed. A video[1] for understanding purposes is linked to this paper. Results and comparison are discussed in Section V.

V. RESULTS

To validate the model proposed in this paper, different force of impacts will be tested. To do so, V_{i_1} from the UR10 robot will variate below its security range of $0.200\ \mathrm{m\,s^{-1}}$. The resulted force of impact and time of collision are deducted from the experiments in the laboratory. These values are compiled in Table II.

[1]Link: short-links.org/r/95lFp

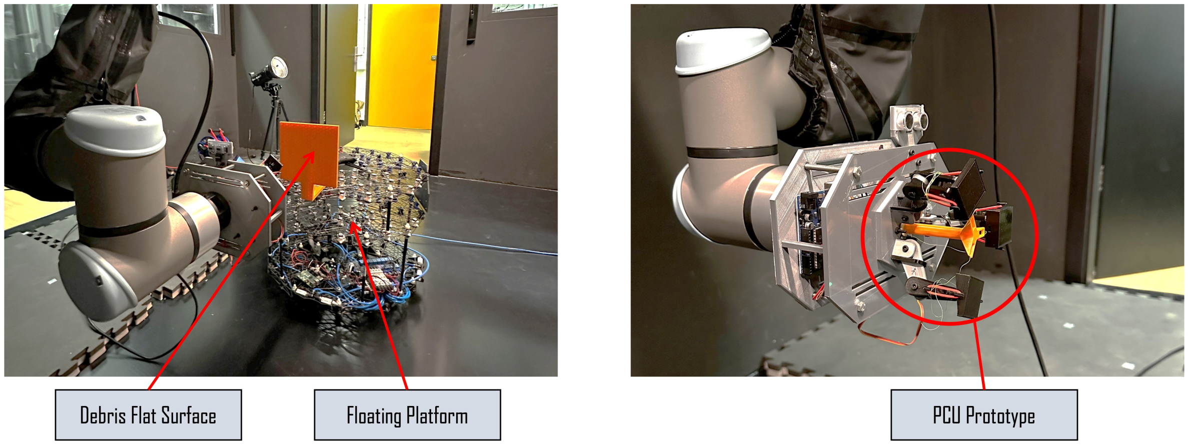

Fig. 5. Experimental setup.

V_{i_1} [m s^{-1}]	$F_{i,Peak}$ [N]	t_c [s]
0.050	3.83	0.320
0.075	4.65	0.302
0.100	6.11	0.327
0.125	6.84	0.380
0.150	6.69	0.393
0.175	6.87	0.373
0.200	6.85	0.367

TABLE II
MODEL INPUTS DEDUCTED FROM THE EXPERIMENTS

The longitudinal deflection L measured in the lab is thus known and compared to the one output from the model, $\hat{L}$. Results are compiled and compared in Table III. The error ϵ is then computed.

V_{i_1} [m s^{-1}]	$L \cdot 10^{-3}$[m]	$\hat{L} \cdot 10^{-3}$ [m]	ϵ [%]
0.050	3.62	3.52	2.76
0.075	5.89	6.09	3.40
0.100	7.51	7.51	0.07
0.125	9.02	8.24	8.65
0.150	15.27	8.11	46.87
0.175	17.77	8.26	53.50
0.200	21.31	8.24	61.33

TABLE III
MODEL OUTPUTS AND TEST COMPARISON

Figure 6 displays the linear deflection of both the tests and the model, function of V_{i_1}. Two sections can be distinguished; a first one where the error is quite small between the model and the experiments, and another one where the error becomes larger and larger. By closely looking at the impact force profiles generated with the experiments, it has been reveled that below 0.150 m s^{-1}, the impact force profile was similar to the one constructed in the model, thus explaining the great performance of the model. However, above this velocity, modelled and experimental impact force profile differ; as the UR10 was continuing its path, it pushed the floating platform with it, creating more than just a perfect pulse. The contact force was decreasing much slower, thus generating biased inputs for the model. In the end, the model is performing great for impact force profile similar to the model, with errors below 3.5%. Improvements and further research on different impact force profile will be conducted.

VI. CONCLUSIONS

In this paper, the mathematical model derived from the mechanical behaviour of the proposed PCU is simulated in MATLAB. Being able to simulate its behaviour under an impact force profile, based on its mechanical properties, brings further the knowledge on the system to safely target a range of flat-surfaced debris. Prototyping the PCU and making it undergo a series of tests in the Zero-G Lab revealed that the model recreates very nicely its dynamic properties; when the impact force profile matches the constructed pulse of the model, the model's error is low. The MATLAB code can be accordingly upgraded to model any other passive compliant system with either longitudinal and/or torsional springs, in different configurations (series or parallel). This paper brings forward the design and knowledge on the Hybrid-Compliant concept for ADR, making research comes closer to autonomously capture a wide range of small debris in orbit, thus contributing to a cleaner space.

VII. FUTURE STUDIES

The presented model's first iteration will improve and get upgrades to recreate the proposed design of the ADR Hybrid-Compliant system. Taking into account higher velocities of approach and different impact force profiles are necessary. Studies of different angle of approach is also needed to assess the design. Moreover, the addition of the ACU behaviour, in the simulation as well as in the laboratory, is an important step towards a technological assessment of the whole concept. Besides, a deeper understanding of the collision will be conducted. To do so, the Coefficient Of Restitution (COR) between the two entities will be investigated. The coefficients of the ACU could be fine-tuned to reduce the COR and get closer to a perfectly inelastic collision. Finally, an experimental validation of the SCU prototype with the

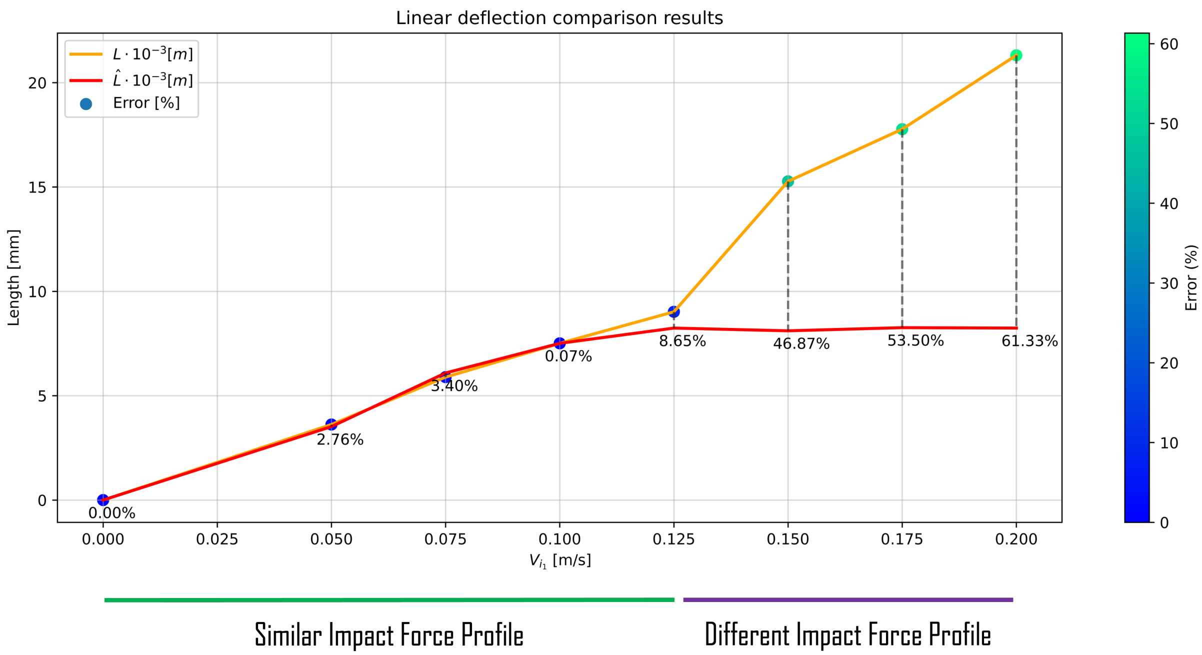

Fig. 6. Linear deflection comparison between the model and the experiments.

dry adhesive is planned in the Zero-G Lab of the University of Luxembourg.

ACKNOWLEDGMENT

This study has been partially funded by Luxembourg National Research Fund (FNR) BRIDGES for "HELEN", project ref: 15836393, and AFR for "CASED", project ref: 16678722. A general overview of Zero-G Lab is available in the following video. The Zero-G Lab has been designed and built to emulate scenarios such as rendezvous, docking, capture between separate spacecrafts [20], [21]. These abilities allow researchers from both industry and academy to conduct a wide variety of experiments for unique orbital scenarios.

REFERENCES

[1] Bernhard, P., Deschamps, M. & Zaccour, G. Large satellite constellations and space debris: Exploratory analysis of strategic management of the space commons. *European Journal Of Operational Research*. **304**, 1140-1157 (2023)

[2] Drmola, J. & Hubik, T. Kessler Syndrome: System Dynamics Model. *In:Space Policy*. pp. 29-39 (2018)

[3] ESA DISCOS, consulted in September 2022. (sdup.esoc.esa.int/discosweb/statistics/)

[4] Liou, J. Active Debris Removal and the Challenges for Environment Remediation. (2012)

[5] Aslanov, V. & Ledkov, A. 2 - Space debris problem. *Attitude Dynamics And Control Of Space Debris During Ion Beam Transportation*. pp. 53-112 (2023)

[6] Bonnal, C. Active debris removal Recent progress and current trends. *Acta Astronautica*. (2013)

[7] Borelli, G., Gaias, G. & Colombo, C. Rendezvous and proximity operations design of an active debris removal service to a large constellation fleet. *Acta Astronautica*. **205** pp. 33-46 (2023)

[8] Yalçın, B., Martinez, C., Delisle, M., Rodriguez, G., Zheng, J. & Olivares-Mendez, M. ET-Class: An Energy Transfer-Based Classification of Space Debris Removal Methods and Missions. *Frontiers In Space Technologies*. **3** pp. 23 (2022)

[9] Kayastha, S., Katupitiya, J., Pearce, G. & Rao, A. Comparative study of post-impact motion control of a flexible arm space robot. *European Journal Of Control*. **69** pp. 100738 (2023)

[10] Viscuso, S., Gualandris, S., De Ceglia, G. & Visentin, V. Chapter 18 - Shape memory alloys for space applications. *Shape Memory Alloy Engineering (Second Edition)*. pp. 609-623 (2021)

[11] Al, N. Ultragentle manipulation of delicate structures using a soft robotic gripper. *Science Robotics*. (2019)

[12] Li, X., Chen, Z. & Wang, Y. Detumbling a Space Target Using Soft Robotic Manipulators. *2022 IEEE International Conference On Mechatronics And Automation (ICMA)*. pp. 1807-1812 (2022)

[13] Feng, L., Martinez, P., Dropmann, M., Ehresmann, M., Ginsberg, S., Herdrich, G. & Laufer, R. MEDUSA – Mechanism for Entrapment of Debris Using Shape memory Alloy. *1st ESA NEO And Debris Detection Conference*. (2019)

[14] Suresh, S. Engineering Gecko-Inspired Adhesives.(https://phowpublished.stanford.edu/cp134gr3166,2020)

[15] Hawkes, E., Jiang, H. & Cutkosky, M. Three-dimensional dynamic surface grasping with dry adhesion. *The International Journal Of Robotics Research*. pp. 1-16 (2015)

[16] Hashizume, J., Huh, T., Suresh, S. & Cutkosky, M. Capacitive Sensing for a Gripper with Gecko-Inspired Adhesive Film. *IEEE Robotics And Automation Letters*. **4** (2019)

[17] Jiang, H., Hawkes, E., Fuller, C., Estrada, M., Suresh, S., Abcouwer, N., Han, A., Wang, S., Ploch, C., Parness, A. & Cutkosky, M. A robotic device using gecko-inspired adhesives can grasp and manipulate large objects in microgravity. *Science Robotics*. **2** (2017)

[18] Hubert Delisle, M., Christidi-Loumpasefski, O., Yalçın, B., Li, X., Olivares-Mendez, M. & Martinez, C. Hybrid-Compliant System for Soft Capture of Uncooperative Space Debris. *Applied Sciences*. **13** (2023), https://www.mdpi.com/2076-3417/13/13/7968

[19] Estrada, M., Hockman, B., Bylard, A., Hawkes, E., Cutkosky, M. & Pavone, M. Free-Flyer Acquisition of Spinning Objects with Gecko-Inspired Adhesives. (http://ieeexplore.ieee.org/document/7487696/,2016)

[20] Al, M. Establishing a Multi-Functional Space Operations Emulation Facility: Insights from the Zero-G Lab. *SSRN*. (2023)

[21] Al, M. Zero-G Lab: A multi-purpose facility for emulating space operations. *Journal Of Space Safety Engineering*. pp. 509 - 521 (2023)

[22] Al., B. Lightweight Floating Platform for Ground-Based Emulation of On-Orbit Scenarios. *IEEE Access*. pp. 94575 - 94588 (2023)

[23] Borchia, D. Torsion Spring Calculator., https://www.omnicalculator.com/physics/torsional-spring.